Journal of Power Sources 205 (2012) 414–419

Contents lists available at SciVerse ScienceDirect

Journal of Power Sources

journal homepage: www.elsevier.com/locate/jpowsour

Highly ordered $LiFePO_4$ cathode material for Li-ion batteries templated by surfactant-modified polystyrene colloidal crystals

Chae-Ho Yim [a], Elena A. Baranova [b], Yaser Abu-Lebdeh [a,*], Isobel Davidson [a]

[a] National Research Council of Canada, 1200 Montreal Road, Ottawa, ON, Canada K1A 0R6
[b] Department of Chemical and Biological Engineering, University of Ottawa, 161 Louis Pasteur, Ottawa, ON, Canada K1N 6N5

ARTICLE INFO

Article history:
Received 8 December 2011
Accepted 2 January 2012
Available online 10 January 2012

Keywords:
$LiFePO_4$
Li-ion battery
Cathode material
Three-dimensionally ordered macroporous structure
Organic template assisted synthesis

ABSTRACT

An organic template assisted synthesis was developed to obtain highly ordered porous $LiFePO_4$ cathode material. The developed synthesis enabled the use of polystyrene (PS) as template by modifying its surface with a surfactant (Brij 78) to render it hydrophilic. The material was synthesized in high yield and purity as confirmed by X-ray powder diffraction. The TEM and SEM images clearly confirmed the presence of a highly ordered porous structure and the latter showed that the structure has an average pore diameter of 400 nm and a wall thickness and depth of ~100 nm. Thermal scans and elemental analysis showed that the material contains a high amount of carbon reaching 23–28% by weight. The surface area was calculated using the BET method and found to be 7.71 $m^2 g^{-1}$. Li/$LiFePO_4$ half cells were tested and gave satisfactory discharge capacities; an initial capacity (158 mAh g^{-1}) close to the theoretical value and recoverable capacities at high C-rates (2–5 C).

1. Introduction

Li-ion batteries are currently used in many consumer electronic products due to their superior performance (e.g. higher energy density and longer cycle life) over other battery technologies [1]. They are therefore under consideration for a wide variety of applications where an energy storage system is needed with most of the attention is focused on transportation [2] and the electrical grid [3]. This requires a further improvement in the performance of the batteries, lower their cost and enhance their safety, which can be achieved by enhancing the functionality of currently used materials or introducing new ones. Cathode materials based on olivine structure $LiMPO_4$ (M: Mn, Fe, Co Ni) are currently considered as a viable alternative to those based on the $LiMO_2$ layered oxide structure, with most of the development is focused on $LiFePO_4$ to replace $LiCoO_2$. $LiFePO_4$ shows a high theoretical capacity ~170 mAh g^{-1} at 3.4 V. It is less toxic, less costly and more environmental friendly than $LiCoO_2$. It is also intrinsically safer due to the strong P—O covalent character of the polyanion (PO_4^{-3}) group that renders the material less prone to oxygen release than layered oxides. The major drawback of $LiFePO_4$ and olivine materials in general is their low intrinsic electronic (~10^{-9} S cm^{-1}) and ionic conductivity (uni-dimensional and/or not normal to the crystalline planes). Several approaches have been suggested to overcome the problem such as introducing carbon as a coating [4] on the surface of the particles or as a composite [5], or "doping" with metal powders [6] or supervalent cations [7] or the formation of iron phosphide networks [8].

Three dimensionally ordered macroporous (3DOM) materials or inverse opals is one type of highly porous materials that attracted a lot of attention in recent years and have been used in a wide range of applications such as in biosensors [9–11], photonics [12–14], and nanofabrications [15]. In batteries, better rate capability was demonstrated with a wide variety of electrode materials that have been synthesized with a 3DOM structure due to faster ionic mobility by providing continuous and very short ionic paths and high surface area for greater contact with the electrolyte. This is mostly done by a soft chemical method that involves impregnation of the inorganic precursor solution into the ordered template that is usually organic in nature like polymers, synthesized by radical polymerization, such as poly(styrene) (PS) or poly(methylmethacrylate) (PMMA) [16], or inorganic such as silica [17]. Also, when the ordered template is removed a structure with closely packed uniformly sized spherical pores (>10 nm) and thick walls (10–100 nm) is formed. In the case when an organic template is used it serves two purposes: besides acting as a template directing the structure into three dimensional order, its thermal decomposition during synthesis leads to the formation of a conductive carbon coating on the surface of the synthesized electrode material, which is very advantageous in the case of olivines.

Recently, Doherty et al. [18] synthesized 3DOM $LiFePO_4$ using a polymethyl methacrylate (PMMA) colloidal template and Lu

* Corresponding author. Tel.: +1 613 949 4184; fax: +1 613 991 2384.
E-mail addresses: Yaser.Abu-Lebdeh@nrc-cnrc.gc.ca, yagal73@yahoo.ca (Y. Abu-Lebdeh).

0378-7753/$ – see front matter.
doi:10.1016/j.jpowsour.2012.01.042

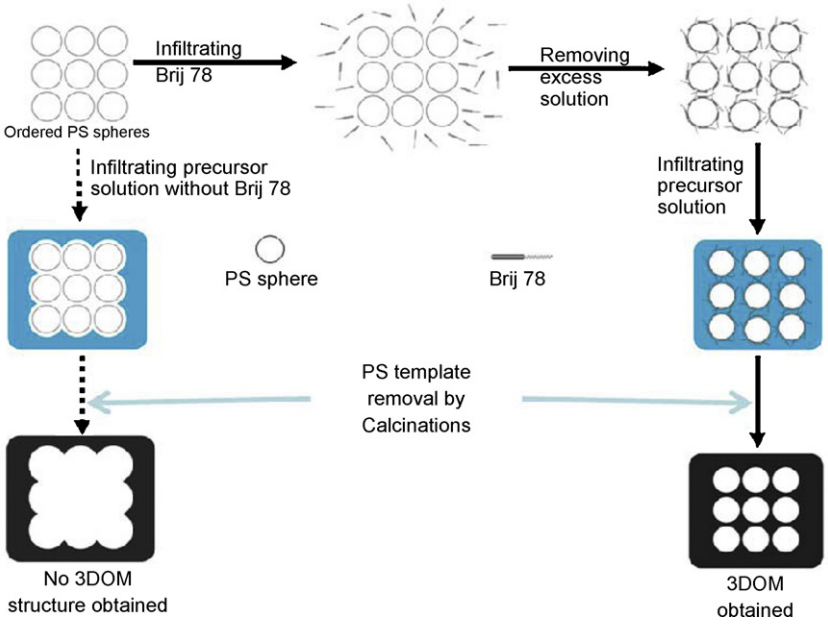

Fig. 1. Schematic of the experimental procedure with and without Brij 78.

et al. [19] using a copolymer of poly(styrene-methyl methacrylate-acrylic acid). The use of PMMA as a colloidal templates was a natural choice due to its hydrophilicity that allows for the infiltration of $LiFePO_4$ aqueous precursor (CH_3COOLi, $Fe(NO_3)_3$, H_3PO_4) solution into its interstitial voids by interacting with the ionic acrylate groups of the polymer. However, it has been demonstrated that the performance of $LiFePO_4$ as a cathode material in Li-ion batteries depends on the amount, type and morphology of the carbon coating that in turn is controlled by the chemistry of the carbon source [20–22]. A wide variety of carbon sources were studied by others to improve the electronic conductivity of olivine materials [21,22]. Nien et al. [22] studied the effect of different types of polymers and found that PS as a carbon source resulted in the highest capacity for $LiFePO_4$. However, PS unlike PMMA is too hydrophobic to allow for the impregnation of the $LiFePO_4$ aqueous precursor solution into its interstitial voids. Although ionic residues from the initiator after polymerization could make it slightly hydrophilic and allow for the synthesis, herein we propose a more effective way to overcome the problem based on the use of a surfactant. Brij 78 is a non-ionic surfactant that contains a long hydrophobic (aliphatic) and hydrophilic (etheric) chain. Infiltration of Brij 78 into the PS template allows for the hydrophobic chain to interact with the surface of the PS and anchoring the surfactant molecules leaving the hydrophilic side free to interact (complex) with the ions in the precursor solution possibly through the ion pairs of etheric oxygens. This will allow for a facile impregnation of the aqueous precursor solution into the interstitial voids of the template.

In this work, the synthesis of 3DOM $LiFePO_4$ assisted by a PS template was successfully possible with very high yield by modifying the surface of PS with a non-ionic surfactant (Brij 78) to enhance its affinity (hydrophilicity) to the aqueous precursor solution. The obtained highly ordered porous $LiFePO_4$ material was characterized by elemental analysis (EDX and XRF), SEM, TEM, TGA, and XRD. Its performance was fully investigated in Li/$LiFePO_4$ half cell batteries (Fig. 1).

2. Experimental

2.1. Synthesis of polystyrene (PS) spheres colloidal template

PS colloids were synthesized by emulsion polymerization, as described by Holland et al. [23]. The styrene monomer was obtained from Sigma–Aldrich (≥99% Reagentplus) and was purged with nitrogen prior to use. Then, 50 mL of styrene was added to 425 mL of de-ionized water, which was also purged with nitrogen. The mixture was heated to 70 °C. To initialize the polymerization, nitrogen-purged aqueous solution of 0.1 M $K_2S_2O_8$ (Sigma–Aldrich, 99%) was added to the mixture. The solution was kept at 70 °C for 24 h under nitrogen. The PS colloids were washed with ethanol (Commercial Alcohols Inc., 95%) and centrifuged at 10000 rpm for 1 h to obtain the ordered organic template, as shown in Fig. 2, Step 1. This step was repeated three times to remove the inorganic impurities. The resulting template was dried in open atmosphere prior to the infiltration of $LiFePO_4$.

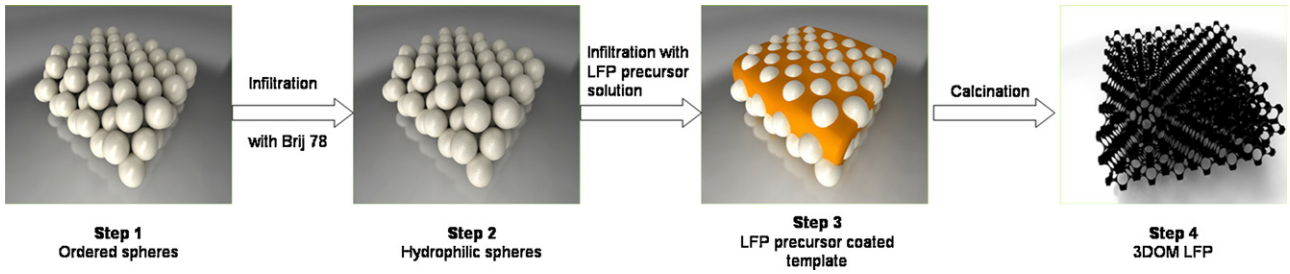

Fig. 2. General synthesis of 3DOM material. Step 1: ordering organic colloids; Step 2: rendering hydrophobicity with Brij 78; Step 3: immersion with precursor solution; and Step 4: calcination to produce 3DOM material.

2.2. Synthesis of $LiFePO_4$

2.2.1. 3DOM $LiFePO_4$

To infiltrate the hydrophilic $LiFePO_4$ precursor solution, the hydrophobicity of the PS template was changed with Brij 78, as shown in Fig. 2, Step 2. First, 0.01 g mL^{-1} of Brij 78 (Sigma–Aldrich) solution was prepared by adding 0.3 g of Brij 78 to 30 mL of ethanol. The PS template was immersed in the Brij 78 solution for 5 min to make sure the Brij is infiltrated into the template. The excess solution was removed using vacuum filtration, and the template was transferred to an alumina boat for further infiltration of the olivine-based precursor solution. The solution was prepared by mixing $LiNO_3$, H_3PO_4 (BDH Inc., 85%), and metal chloride, $FeCl_2{\cdot}4H_2O$ (Alfa Aesar, 98%) in distilled water. The precursor solution was prepared to yield 1 g of the olivine-based material. The metal chloride was fully dissolved in 1 g of water, and H_3PO_4 and $LiNO_3$ were added and mixed until the salts were fully dissolved. The precursor solution of the olivine-based material was infiltrated into the template. A pipette was used to slowly coat the template with the solution, as shown in Fig. 2, Step 3. The infiltrated template was allowed to dry overnight. Then, the dry organic template was sintered under argon (Linde Canada, 99.999%). Calcinations were performed in two stages under argon: once at 260 °C for 3 h to remove the PS template from the olivine-based materials and again at 700 °C for 3 h to obtain the olivine-based materials with a carbon coating. To prevent the volatile decomposition of the PS template, a slow temperature rate of 2 °C min^{-1} was used.

2.2.2. Standard non-templated $LiFePO_4$/C

A solid-state reaction was used to synthesize $LiFePO_4$ (LFP). Li_2CO_3 (Sigma–Aldrich, 99%), $Fe(C_2H_3O_2)_2{\cdot}2H_2O$ (Riedel deHaen, 99%), and $NH_4H_2PO_4$ (Sigma–Aldrich, 99%) were mixed in a molar ratio of 0.5:1:1. Citric acid was added to the mixture to carbon coat the LFP. The amount of citric acid was 5 wt% of final synthesized LFP. The mixture was soft ball milled using 60 mL of NALGENE jar (VWR) with zirconia beads (Tosoh Corp., 5 mm in diameter) for homogenous mixing. Enough acetone to fill half of the NALGENE jar was added to the mixture with 20 zirconia beads. The mixture was ball milled for three days and then acetone was evaporated under the fume hood. The remaining mixture was sintered under argon at 700 °C.

2.3. Characterization of PS and 3DOM $LiFePO_4$

Powder X-ray diffraction was carried out between 15° and 85° (2θ angles) using a Bruker AXS D8 diffractometer with a Co Kα source with 35 kV and 45 mA of power, a divergence angle of 0.3°, a step size of 0.027°, and an acquisition time of 1 s per step. The patterns were analyzed by the Rietveld refinement method [24] using the software TOPAS v4.2 from Bruker AXS [25]. The morphology of the material was characterized by scanning electron microscopy (SEM) using a JEOL 840A. Thermal gravimetric analysis (TGA) was performed to quantify the amount of carbon present in the 3DOM $LiFePO_4$. A TGA 2950 TA instrument was used. The composite was heated at 10 °C min^{-1} up to 110 °C for 30 min to remove moisture contained in the material and then heated continuously up to 800 °C in air in order to oxidize the carbon from the composite.

The elemental analysis technique, X-ray fluorescence (XRF) analysis, was performed using an automated Bruker AXS S4 Pioneer. The S4 pioneer is a 4 kW sequential wavelength-dispersive XRF spectrometer using an Rh-anode X-ray tube with 75 μm thin Be end window. All the measurements were done under vacuum mode using a 28 mm mask and a 0.23° collimator. The sample was prepared by the lithium borate fusion method. 100 mg of sample was mixed with 7 g of flux. The type of flux used was Claisse, which is made of 66.67% of $Li_2B_4O_7$, 32.83% of $LiBO_2$, and 0.5% of LiBr. The mixtures were fused with a Claisse M4 three-position gas fluxer producing 32-mm glass beads at 1000 °C.

Transmission electron microscopy (TEM) analysis of 3DOM $LiFePO_4$ was carried out using a JEOL JEM 2100F FETEM microscope operating at 120 kV. The sample was prepared for TEM analysis by sonicating and suspending the 3DOM $LiFePO_4$ in ethanol. Copper grid was dipped to the sample solution several times and dried on air. Bulk elemental composition of the resulting 3DOM $LiFePO_4$ deposited on carbon support was studied using energy dispersive X-ray analysis (EDX). The EDX analysis was performed using a JEOL JSM-7500F field emission scanning electron microscope equipped with an energy dispersive X-ray spectrometer (Oxford Instrument). The spectra were acquired at an acceleration voltage of 20 kV.

The specific surface area was estimated by nitrogen adsorption–desorption porosimetry at 77 K via the Brunauer–Emmet–Teller (BET) method. The instrument employed was a Micromeritics ASAP2000 system. Prior to each measurement, the sample was evacuated overnight at 150 °C under a pressure, 10^{-6} Torr.

2.4. Lithium battery performance of 3DOM $LiFePO_4$ in Li-ion cell

3DOM $LiFePO_4$ was tested as a Li-ion half-cell using a 2325-type coin cell. The electrode was prepared from a slurry made of 75 wt% active material, 5 wt% carbon Super S (Timcal graphite and Carbon, Switzerland), 5 wt% carbon graphite E-KS4 (KG, Lonza G+T, Switzerland) and 15 wt% of polyvinylidene fluoride (PVDF, Kynar Flex 2800 dissolved in N-methyl-pyrrolidone from Aldrich) as a binder. The cast was prepared using an automated doctor blade spreader and dried overnight in a convection oven at 85 °C, and then in a vacuum oven overnight at 80 °C. Individual electrodes (Ø = 12.5 mm) were punched out, dried at 80 °C under vacuum overnight, pressed under a pressure of 0.5 metric ton, and were used as positive electrodes. A lithium disk (Ø = 16.5 mm) was used as a negative electrode (counter electrode and reference electrode). 70 μL of 1 M $LiPF_6$ in EC:DMC (1:1 by volume) was used as electrolyte and spread over a double layer of the polypropylene separators (Celgard 30). The batteries were assembled in an argon-filled dry box. The cells were cycled galvanostatically using an Arbin battery cycler and tested using cyclic voltammetry techniques. The cells were tested at different C-rates of charge/discharge: C/12, C/6, C, 2 C and 5 C. Five full cycles of charge/discharge were measured for each C-rate.

3. Results and discussion

A white powder of PS spheres was obtained by centrifugation of the milky solution at the end of polymerization reaction of styrene, separation of ordered PS template from the solution and drying the PS template. Coating the powder with Brij 78 followed by impregnation with precursor solution and calcinations gave a black $LiFePO_4$ powder. Fig. 3 shows the Rietveld refinement of the synthesized $LiFePO_4$ powder with the reference peaks for $LiFePO_4$ (ISCD 161479) shown as black lines right above the *x*-axis. The XRD patterns show a pure $LiFePO_4$ phase with no evidence of any other phases or impurities. The space group of $LiFePO_4$ was identified as *Pmna* with a crystal size of 78.1 nm and the lattice parameters are determined and listed in Table 1. The parameter values and crystal structure agree very well with the results described in the literature [18,26–28]. The reference peaks are used to simulate the fit in order to evaluate the lattice parameter and crystal size using the software TOPAS v4.2.

The surface area of the composite was measured using the BET method. It was found to be 7.71 $m^2\,g^{-1}$ which was much lower than that for $LiFePO_4$ synthesized by Doherty et al. (~50 $m^2\,g^{-1}$)

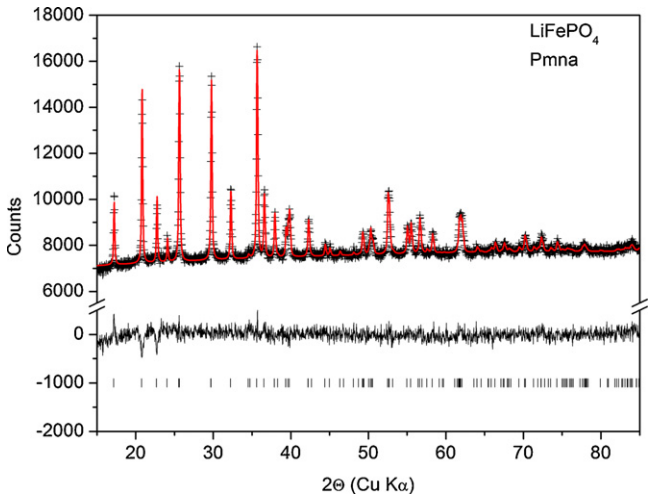

Fig. 3. Rietveld refinement of the X-ray diffraction pattern of the 3DOM $LiFePO_4$.

Table 1
Lattice parameters of synthesized and reference $LiFePO_4$.

Lattice parameters	Synthesized	Ref. [32]
a (Å)	10.3331 (5)	10.33
b (Å)	6.0106 (3)	6.01
c (Å)	4.6953 (3)	4.70
Crystal size (nm)	78.1 (2)	N/A

[18], and a little smaller than the $LiFePO_4$ synthesized by Phostech Lithium Inc. (12 $m^2\ g^{-1}$) [29]. It is known that the amount of carbon in $LiFePO_4$/C composite affects greatly the surface area of $LiFePO_4$; the higher the amount of carbon the lower the surface area [18]. This could be attributed, among other things, to the fact that the carbon content in the composite interferes in the 3D porous network and blocks some of the paths hence isolating large surfaces from the accessible total surface area of $LiFePO_4$.

Fig. 4 shows the SEM micrographs of the synthesized $LiFePO_4$ with a Brij 78-coated PS template and the unmodified PS template. From the inset image, it can be seen that PS template has average sphere diameters in the range between 300 and 500 nm closely packed in an orderly fashion. The main image shows a macroporous structure of $LiFePO_4$ with overlaid layers and ordered pores in a simple cubic structure having a diameter that matches those of the spheres of the PS template. The thickness and the depth of

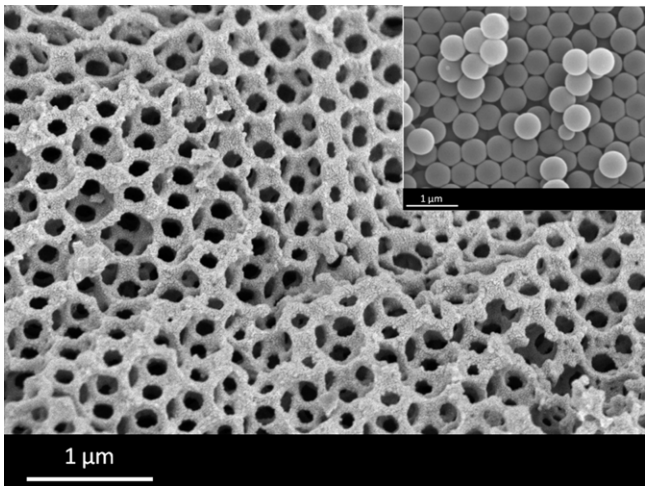

Fig. 4. SEM micrograph of the synthesized 3DOM $LiFePO_4$ and PS colloids (inset).

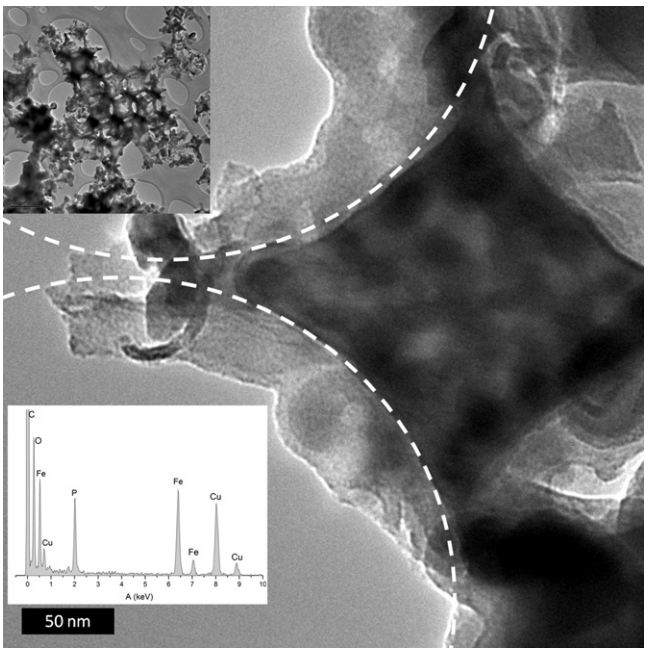

Fig. 5. TEM micrograph of the synthesized 3DOM $LiFePO_4$.

the synthesized 3DOM $LiFePO_4$ are similar as it is the case for cubic structures and can be approximately estimated to be in the range of 100 nm. In some parts of the image, ruptures in the structure can be easily seen that could be attributed to the volatile decomposition products of some chains of the PS template. The procedure was repeated to ensure that the synthesis of 3DOM $LiFePO_4$ could be reproduced and the same morphology (SEM) and XRD diffraction pattern were observed. Fig. 5 shows TEM micrographs of the synthesized $LiFePO_4$. The images show clearly an open structure with a regular void pattern that resembles the one observed in the SEM images. The enlarged image shows part of the 3DOM structure with $LiFePO_4$ core (dark region) surrounded by the edges of the spherical voids covered by a carbon coating (bright region) that is 50 nm or less thick. The white dashed lines shown are the trace of the spherical voids. The second inset is an EDX scan of the same 3DOM $LiFePO_4$ sample. The scan shows all the expected elements in the composites: Fe, P, O, C, except for Li that could not be observed due to the limit of the EDX. Cu from the sample holder can also be seen.

Brij 78 was used to render PS template hydrophilic to allow for the infiltration of the concentrated aqueous precursor solution that is necessary to obtain high yield of the 3DOM material. The highly concentrated precursor solution (1 g of water) has difficulty infiltrating into the interstitial voids of the hydrophobic PS template when no modification of surface was made. In fact, the precursor solution formed a large convex meniscus on top of the PS template and when left to dry turned into lumps of yellow spots distributed unevenly at the surface. The Brij 78 surfactant consists of long etheric hydrophilic and aliphatic hydrophobic blocks. The hydrophobic blocks bound with the PS colloids while the hydrophilic blocks standing out of the colloids to allow for infiltration of the water-based precursor solution. This was achieved by immersing the dry PS template in a solution of Brij 78 in ethanol. The powder broke into millimeter-sized particles associated with small bubbles originating from air trapped among the interstitial voids of the templates. After 2 min, the fine bubbles could no longer be observed, indicating the completion of the infiltration. To complete the infiltration of the Brij solution, it was left still for few more minutes with total infiltration time of approximately 5 min. The excess Brij solution was removed using vacuum filtration. When

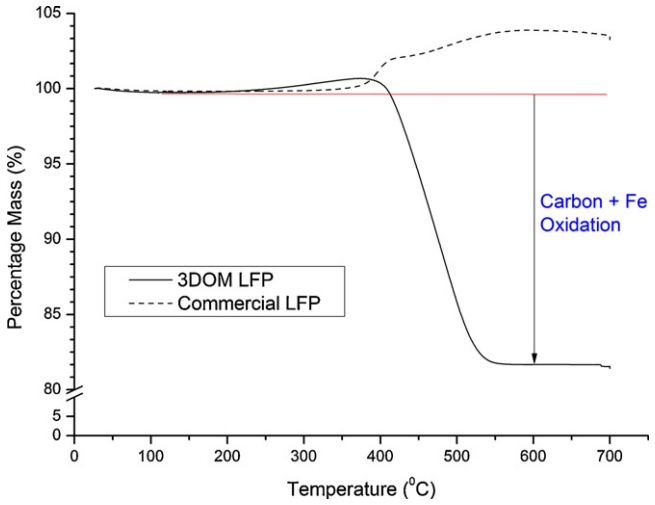

Fig. 6. TGA analysis of $LiFePO_4$ under oxygen.

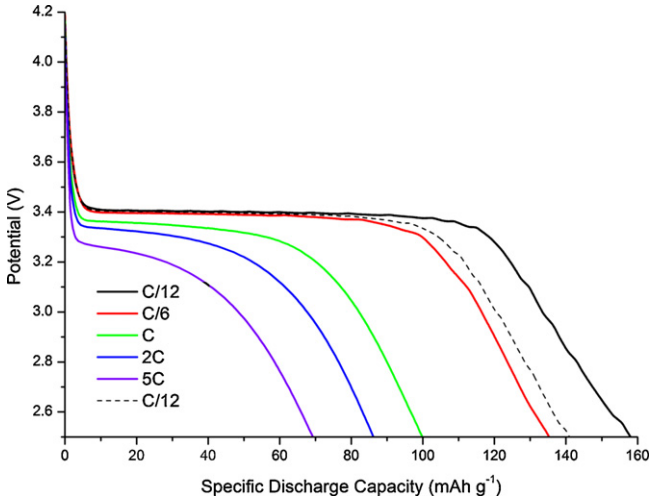

Fig. 7. Discharge curves of 3DOM $LiFePO_4$ at different C-rates.

Brij 78 was coated onto the template, the infiltration period for the aqueous precursor solution was short and it was homogenously infiltrated through the PS template.

Two-step calcination at very slow heating rate was performed in order to remove the PS colloids while maintaining the 3DOM structure by preventing the volatile decomposition of PS colloids and to give enough time for the inorganic materials to condense and react. In the first step, calcination occurred at 260 °C for 3 h in order to remove the PS template and condense the material, while in the second step calcination occurred at 700 °C for another 3 h in order to synthesize and crystallize the $LiFePO_4$. At the end of the calcinations the synthesized materials were left to cool down slowly to room temperature. The calcinations were performed under inert atmosphere (argon) to prevent the oxidization of Fe^{2+} to Fe^{3+}, and also to allow for the formation of carbon coating on the materials instead of forming gasses.

Fig. 6 shows the thermal gravimetric analysis (TGA) curve of $LiFePO_4$ heated in air. TGA was performed under air to oxidize and decompose the entire carbon residue in the material. TGA is commonly used for evaluating the carbon content [27]. Based on the results, the commercial $LiFePO_4$ had 3% weight gain, suggesting 1 wt% of carbon in the active material, when 5% weight gain is assumed to be the result of $LiFePO_4$ oxidation. The synthesized $LiFePO_4$ in this work showed 19% weight loss, that corresponds to 23 wt% of carbon content in the $LiFePO_4$. At high temperatures and pressure, Fe (II) in $LiFePO_4$ gets oxidized to Fe (III) (Eq. (1)), as suggested by Belharouak et al. [27]:

$$LiFePO_4 + (1/4)O_2 \rightarrow (1/3)Li_3Fe_2(PO_4)_3 + (1/6)Fe_2O_3 \quad (1)$$

As a result of this oxidation, weight gain of 5% was observed due to the reaction of oxygen with iron cation in $LiFePO_4$. The same calculation was made using the TGA results. As the oxidation occurs at high temperature that follows the same reaction path as Eq. (1), using the initial and final weights, the carbon contents in the materials were evaluated and found to be 23 wt%. XRF was used to verify the amount of carbon content. During the sample preparation 28 wt% loss was observed, due to the loss of carbon residues in the composite and therefore the total amount of carbon in the sample. The value is slightly higher compared to the one obtained by TGA (23 wt%). Also, the atomic ratio of the composite was confirmed to be 1:1:4 for Fe:P:O, which is the exact composition ratio of $LiFePO_4$.

The effect of the amount and type of carbon coating on the performance of $LiFePO_4$ has not yet been fully studied. However, a thin layer is only necessary in order to allow for the diffusion/migration of Li ions in and out of $LiFePO_4$ and less than 5 wt% seems sufficient even at high charge/discharge rates. The calculated amount of carbon (23 wt%) in our material is very high due to the nature of PS decomposition where less depolymerization versus side chain decomposition takes place at the initial stage of calcination. This allows for the formation of higher molecular weight carbon precursor instead of the loss of material by the formation of volatile low molecular weight, depolymerized monomer-like species. Also, in our synthetic method the decomposition products of the Brij 78 surfactant contribute to the amount of carbon coating. Moreover, the type of the carbon formed in our case is believed to be highly conductive as pointed out by Nien et al. [22] who showed that PS makes highly conductive carbon coatings on $LiFePO_4$ due to the fact that it contains an aromatic phenyl group. Organic (molecular or polymeric) compounds with aromatic moieties have been investigated as a carbon precursor during the synthesis of $LiFePO_4$ due to their ability to form a highly graphitic type of carbon that is more electronically conductive [20,27].

Fig. 7 shows the discharge curve of the synthesized $LiFePO_4$ that was tested as a cathode in a half-cell while lithium metal was used as an anode electrode. It shows the typical flat discharge curve of $LiFePO_4$ indicative of two-phase reaction of $LiFePO_4/FePO_4$ according to: $LiFePO_4 \rightarrow FePO_4 + Li^+ + e^{-1}$. The initial discharge capacity at C/12 was found to be 158 mAh g^{-1} that is close to the theoretical capacity of 170 mAh g^{-1} [26]. The first discharge curves at different C-rates are also shown. It can be seen that at high discharge C-rate the flat plateau is shortened and the inclined drop in potential dominates due to diffusion polarization (mass transport step slower than the other steps in the electrochemical reaction). The presence of a highly porous structure in the $LiFePO_4$ cathode seems to have little effect in mitigating the effect of diffusion polarization on the electrochemical performance of $LiFePO_4$ which is due to the large carbon content in the material. Similar behavior was observed by Doherty et al. [18] who reported slightly lower capacities (140 mAh g^{-1} at C/10 and 70 mAh g^{-1} at 5 C) for the $LiFePO_4$ templated by PMMA (spheres with diameter 270 nm) and has carbon content of 7 wt% synthesized at 700 °C. They suggested that excess carbon seems to block Li ion movement through the interface and the electrolyte molecules and ions through the pores. Similar behavior was also reported by many others in nano-sized $LiFePO_4$ particles (~100 nm) and it is widely accepted that low carbon content (3.2 wt%) with porous structure and very high conductivity (sp^2 character) is sufficient to allow for electrons to reach the electro-active sites in $LiFePO_4$, therefore making it suitable for

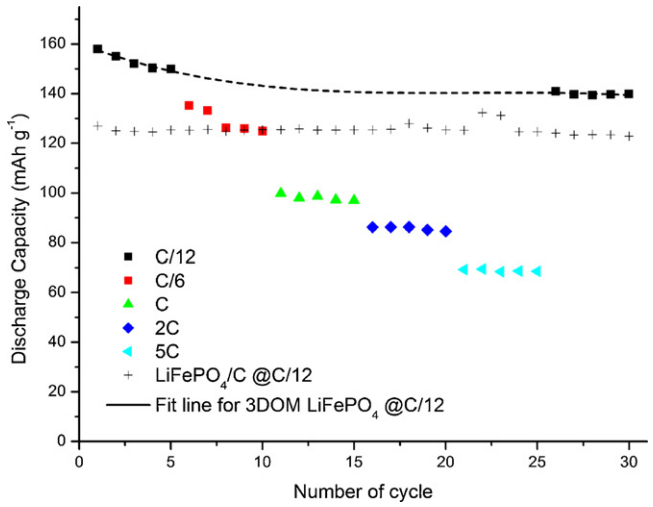

Fig. 8. Specific capacity of 3DOM $LiFePO_4$ at different C-rates.

high power applications. It is also worth mentioning that the high amount of carbon has also a large negative effect on the volumetric energy density of the battery. Using a density value of 2.2 g cm^{-3} for carbon and 3.6 g cm^{-3}, we can calculate a 0.7 Wh cm^{-3} drop of energy density (from 2.1 to 1.4 Wh cm^{-3}) at a carbon content of 23 wt%. In general, we can see that the high amount of carbon, although of the more conductive graphitic type, has a negative effect on the electrochemical and battery performance of $LiFePO_4$ but different approaches are under consideration to lower the amount of carbon such as: sintering the material in different gas composition in hydrogen and steam that are commonly used to purify carbon nanotubes [30]; or using different sizes of PS spheres [18].

Fig. 8 shows the specific discharge capacity of the synthesized $LiFePO_4$ tested at different C-rates. Five cycles were repeated at each C-rate: C/12, C/6, C, 2 C, 5 C, and back to C/12 again to check for any capacity fade after high C-rate cycling. During the first 10 cycles (at C/12 and C/6), capacity fade of 6% was observed that is commonly associated with increased resistances at the interface and the bulk electrode, with the former being more significant in this case due to the high surface area of the material [31]. After the tenth cycle, the capacity was stabilized and also recovered at low C-rate (C/12) with a 12% loss from the initial capacity (158 mAh g^{-1}). For comparison, standard non-templated carbon-coated $LiFePO_4$ was synthesized and tested in a half cell battery and the results are also shown in Fig. 8. The discharge capacity at C/12 for 3DOM $LiFePO_4$ has been fitted using the first and last five cycles and were calculated based on weight of $LiFePO_4$ in the composite. Using the fitted line the capacity could be compared to the standard $LiFePO_4$. As shown in the figure, the capacity is ~20 mAh g^{-1} higher for 3DOM $LiFePO_4$ sample due to the greater access of lithium in the porous structure.

4. Conclusions

Three dimensionally ordered macroporous $LiFePO_4$ was successfully synthesized by means of a new organic template-assisted synthesis. The polystyrene polymer synthesized as spheres in 300–500 nm diameters was ordered successfully to make the template. The surfactant Brij 78 was used to render the surface of the spheres hydrophilic to allow for the infiltration of precursor solution. Upon calcinations, pure phase in high yield of the $LiFePO_4$ with a crystal size of 78.1 nm was successfully achieved as evidenced by XRD patterns and the ordered macrostructure was clearly seen by SEM and TEM images. Carbon content was estimated at 23–28 wt% of the material. The resulting 3DOM $LiFePO_4$ material showed a satisfactory battery performance that was clearly affected by the high amount of carbon yet still higher than the non-templated sample; it showed a discharge capacity of 158 mAh g^{-1} recoverable after long and high C-rate cycling.

References

[1] M. Armand, J.M. Tarascon, Nature 451 (2008) 652–657.
[2] G. Gutmann, Encyclopedia of Electrochemical Power Sources, Elsevier, Amsterdam, 2009, pp. 219–235.
[3] Z. Yang, J. Zhang, M.C.W. Kintner-Meyer, X. Lu, D. Choi, J.P. Lemmon, J. Liu, Chem. Rev. 111 (2011) 3577–3613.
[4] N. Ravet, Y. Chouinard, J.F. Magnan, S. Besner, M. Gauthier, M. Armand, J. Power Sources 97–98 (2001) 503–507.
[5] H. Huang, S.C. Yin, L.F. Nazar, Electrochem. Solid-State Lett. 4 (2001).
[6] F. Croce, A. D'Epifanio, J. Hassoun, A. Deptula, T. Olczac, B. Scrosati, Electrochem. Solid-State Lett. 5 (2002) A47–A50.
[7] S.Y. Chung, J.T. Bloking, Y.M. Chiang, Nat. Mater. 1 (2002) 123–128.
[8] P.S. Herle, B. Ellis, N. Coombs, L.F. Nazar, Nat. Mater. 3 (2004) 147–152.
[9] J.M. Weissman, H.B. Sunkara, A.S. Tse, S.A. Asher, Science 274 (1996) 959–960.
[10] C.E. Reese, M.E. Baltusavich, J.P. Keim, S.A. Asher, Anal. Chem. 73 (2001) 5038–5042.
[11] T. Cassagneau, F. Caruso, Adv. Mater. 14 (2002) 1629–1633.
[12] W. Cheng, J. Wang, U. Jonas, G. Fytas, N. Stefanou, Nat. Mater. 5 (2006) 830–836.
[13] J.D. Joannopoulos, P.R. Villeneuve, S. Fan, Nature 386 (1997) 143–149.
[14] E. Yablonovitch, Sci. Am. 285 (2001) 34–41.
[15] U.C. Fischer, H.P. Zingsheim, J. Vac. Sci. Technol. 19 (1981) 881–885.
[16] J.C. Lytle, H. Yan, N.S. Ergang, W.H. Smyrl, A. Stein, J. Mater. Chem. 14 (2004) 1616–1622.
[17] A. Stein, R.C. Schroden, Curr. Opin. Solid State Mater. Sci. 5 (2001) 553–564.
[18] C.M. Doherty, R.A. Caruso, B.M. Smarsly, C.J. Drummond, Chem. Mater. 21 (2009) 2895–2903.
[19] J. Lu, Z. Tang, Z. Zhang, W. Shen, Mater. Res. Bull. 40 (2005) 2039–2046.
[20] M.M. Doeff, Y. Hu, F. McLarnon, R. Kostecki, Electrochem. Solid-State Lett. 6 (2003) A207–A209.
[21] R. Dominko, M. Bele, M. Gaberscek, M. Remskar, D. Hanzel, S. Pejovnik, J. Jamnik, J. Electrochem. Soc. 152 (2005).
[22] Y.H. Nien, J.R. Carey, J.S. Chen, J. Power Sources 193 (2009) 822–827.
[23] B.T. Holland, C.F. Blanford, T. Do, A. Stein, Chem. Mater. 11 (1999) 795–805.
[24] H. Rietveld, Acta Crystallogr. 22 (1967) 151–152.
[25] BrukerAXS, Inc., Karlsruhe, Germany, 2008.
[26] A.K. Padhi, K.S. Nanjundaswamy, J.B. Goodenough, J. Electrochem. Soc. 144 (1997) 1188–1194.
[27] I. Belharouak, C. Johnson, K. Amine, Electrochem. Commun. 7 (2005) 983–988.
[28] D. Jugovic, D. Uskokovic, J. Power Sources 190 (2009) 538–544.
[29] Phostech Lithium Inc., http://www.phostechlithium.com/prd_LiFePO4P1_e.php, December 7, 2011.
[30] G. Tobias, L. Shao, C.G. Salzmann, Y. Huh, M.L.H. Green, J. Phys. Chem. B 110 (2006) 22318–22322.
[31] H. Duncan, Y. Abu-Lebdeh, I.J. Davidson, J. Electrochem. Soc. 157 (2010).
[32] M.S. Song, Y.M. Kang, Y.I. Kim, K.S. Park, H.S. Kwon, Inorg. Chem. 48 (2009) 8271–8275.